European Journal of Neuroscience, Vol. 27, pp. 396–407, 2008 doi:10.1111/j.1460-9568.2007.06010.x

The axon-guidance *roundabout* gene alters the pace of the *Drosophila* circadian clock

Jimena Berni, Esteban J. Beckwith, María Paz Fernández and María Fernanda Ceriani
Laboratorio de Genética del Comportamiento, Fundación Instituto Leloir, Instituto de Investigaciones Bioquímicas-Buenos Aires (IIBBA, CONICET), Av. Patricias Argentinas 435, Buenos Aires 1405, Argentina

Keywords: circadian rhythms, *Drosophila*, PDF, *roundabout*, short period, synchronization

Abstract

Great efforts have been directed to the dissection of the cell-autonomous circadian oscillator in *Drosophila*. However, less information is available regarding how this oscillator controls rhythmic rest–activity cycles. We have identified a viable allele of *roundabout*, $robo^{hy}$, where the period of locomotor activity is shortened. From its role in axon-pathfinding, we anticipated developmental defects in clock-relevant structures. However, $robo^{hy}$ produced minor defects in the architecture of the circuits essential for rhythmic behaviour. ROBO's presence within the circadian circuit strengthened the possibility of a novel role for ROBO at this postdevelopmental stage. Genetic interactions between pdf^{01} and $robo^{hy}$ suggest that ROBO could alter the communication within different clusters of the circadian network, thus impinging on two basic properties, periodicity and/or rhythmicity. Early translocation of PERIOD to the nucleus in $robo^{hy}$ pacemaker cells indicated that shortened activity rhythms were derived from alterations in the molecular oscillator. Herein we present a mutation affecting clock function associated with a molecule involved in circuit assembly and maintenance.

Introduction

Rhythmic locomotor behaviour in *Drosophila* depends primarily on the rhythmic activity of a group of neurons known as the small ventral lateral neurons (LNvs), present in both brain hemispheres (Helfrich-Forster, 1998). These neurons are located close to the accessory medulla and send their projections dorsally towards the superior protocerebrum, ending close to other circadian relevant groups: the dorsal neuron (DN) clusters 1, 2 and 3 (Helfrich-Forster, 1997; Kaneko & Hall, 2000). The circadian network also includes a group of about six neurons located dorsally from the sLNvs known as lateral neurons dorsal (LNd). The small LNvs release a neuropeptide called pigment dispersing factor (PDF), and this release in the dorsal protocerebrum is impaired in certain clock mutants (Park *et al*., 2000; Lear *et al*., 2005a; Fernandez *et al*., 2007). Under constant darkness (a condition that allows the endogenous circadian clock to become apparent) the oscillation in PDF immunoreactivity remains rhythmic with a period close to 24 h (Park *et al*., 2000). This rhythmicity under free-running conditions depends on both an intact molecular oscillator and an intact circadian circuitry (Helfrich-Forster, 2003). Recently, the hierarchy of the small LNvs over certain dorsal clusters has been demonstrated (Stoleru *et al*., 2005). At the molecular level, rhythmic behaviour is the result of the concerted action of a number of clock genes whose mRNA, protein levels and/or activity change throughout the day in a circadian fashion (Hardin, 2005).

Axonal growth cones find their way through a careful evaluation of multiple attractive and repulsive cues (Goodman, 1996). In *Drosophila,* the *roundabout* (*robo*) family of Ig transmembrane receptors is crucial for proper axon guidance during embryogenesis (Seeger *et al*., 1993; Kidd *et al*., 1998a), and cell migration and positioning at later stages (Kramer *et al*., 2001; Jhaveri *et al*., 2004). ROBO is expressed at the growth cone filopodia and respond to the repulsive diffusible ligand SLIT emanating from the midline (Kidd *et al*., 1999; Rajagopalan *et al*., 2000; Simpson *et al*., 2000). Growth cone repulsion mediated by SLIT-triggered ROBO signalling appears to be common to different circuit designs. Overexpression of ROBO in the giant fibre circuit interferes with synaptic function and affects the establishment of the circuit (Godenschwege *et al*., 2002).

Recently Jhaveri *et al*. (2004) showed that lack of ROBO function during puparium formation leads to defects in the position of sensory terminals as well as the formation of the commissures connecting the two olfactory lobes in *Drosophila*. Likewise, SLIT-mediated ROBO signalling is crucial to determine proper compartmentalization of certain regions within the developing *Drosophila* eye (Tayler *et al*., 2004). In this study we report the identification of a *roundabout* mutation that shortens the period of rest–activity cycles. We named it $robo^{hypomorph}$ ($robo^{hy}$) as it expressed roughly half the amount of ROBO compared to matched controls for genotype and age. Despite the anticipated role in circuit assembly, the PDF network displayed only subtle defects in the axon trajectory. ROBO detection in the adult CNS suggests a potential acute role of ROBO at this stage. Genetic interactions with PDF, the only synchronizing cue so far described in the circadian network, underscores that ROBO could modulate the signalling downstream of the small LNvs Noteworthy, the period-shortening defect in locomotor behaviour correlates with an earlier entry of PERIOD (PER) to the nucleus in pacemaker cells, further supporting the notion that the circadian network feedbacks onto the molecular oscillator operating within the small LNv cluster (Stoleru *et al*., 2004).

Correspondence: Dr María Fernanda Ceriani, as above.
E-mail: fceriani@leloir.org.ar

Received 5 June 2007, revised 19 November 2007, accepted 22 November 2007

Materials and methods

Fly strains

Wild-type w^{1118} and w^{1118}; *robo*^{BG1092} (renamed *robo*^{hy}), UAS-ANF-green fluorescent protein (GFP), UAS-CD8-GFP and *tim*-gal4 were obtained from the Bloomington Stock Center. *robo*^{1} is described in (Kidd *et al*., 1998a); 2XUAS-*robo-myc* is described in Godenschwege *et al*. (2002). *pdf*^{01} flies were provided by Orie Shafer (P. Taghert's laboratory). For locomotor activity experiments flies were grown and maintained at 25 °C in vials containing standard cornmeal medium under 12 : 12 h light : dark cycles, with an average light intensity of 36 photon micromoles m^{-2} s^{-1} (measured with a Quantum Meter model QMSW-SS; Logan, UT, USA). Flies were typically 1–5 days old at the onset of locomotor behaviour analysis or dissection.

A P-element mobilization strategy was used to remove the original transposon (BG1092), via the transient introduction of the transposase (Δ2–3), and created stocks of each excision event. Backcrosses to *robo*^{hy} minimized background effects which could contribute to period differences in the locomotor activity experiments. PCR reactions on genomic DNA obtained from a number of independent white-eyed flies were performed with primers lying on exon 1 (ACC CAC GTC CAA TTG TGA GT) and exon 5 (GGT GTG TGA GTG TCC AAG TGT G) of the *robo* locus. Sequencing reactions allowed the identification of precise excisions.

Locomotor behaviour analysis

Newly eclosed flies were entrained to 12 h light–dark (LD) cycles for 3 days, and adult males were placed in glass tubes and monitored for activity with infrared detectors and a computerized data collection system (TriKinetics). Activity was monitored in LD conditions for 3–4 days and then the flies were released into constant darkness (DD) for at least 1 week. Data were analysed using the Clocklab software package (Actimetrics, Evanston, IL, USA). Periodogram analysis of flies that were scored as arrhythmic produced no strong peak that was statistically significant ($P < 0.05$). Those flies that showed recognizable daily onsets and ends of activity that was not consolidated, thus resulting in periodograms that displayed weakly significant periods, were classified as weakly rhythmic (Yang & Sehgal, 2001; Ceriani *et al*., 2002) and were not taken into account for average period calculations.

Olfaction

Wild-type and *robo*^{hy} females and males were starved for 4–6 h and then tested in groups of five in a quantitative olfactory paradigm against 5 μL of 50 μM benzaldehyde or water as in Anholt *et al*. (1996). Ten readings were obtained from each individual group. Experiments were performed twice with similar results. Statistical analysis (one-way ANOVA with a Bonferroni *post hoc* test) was employed to assess significance.

Eclosion

Emergence from the puparium was recorded at 25 °C employing an automated setup (Trikinetics, Waltham, MA, USA). Pupae synchronized to 12-h LD cycles kept at 20 °C were glued to the plates and transferred to DD 3–4 days before ecdysis. To extend the monitoring interval (and have a better assessment of the endogenous period for each line) plates were replenished every 3 days (twice per experiment) from bottles transferred to DD at the onset of the experiment. Experiments were performed five or six times with similar results.

Western blot analysis

Protein extracts were prepared from adult heads or embryos. Fifty microgrammes of total protein was loaded per lane. Lysis was performed in 20 mM Tris-HCl, 100 mM NaCl, 1 mM EDTA and 2 mM DTT in the presence of a protease inhibitor cocktail (Sigma). Soluble protein extracts were separated on 6% polyacrylamide electrophoresis gels, transferred to supported nitrocellulose membranes (MSI, Westboro, MA) and incubated with anti-ROBO (1 : 100; 13C9 Developmental Studies Hybridoma Bank; Kidd *et al*., 1998a) or anti-HSP70 (1 : 5000; Sigma) antibodies. Goat antirabbit or anti-mouse conjugated to horseradish peroxidase were employed at 1 : 5000 (Jackson Immunoresearch). Chemiluminescent detection was used to develop the reaction (ECL+ Amersham).

Dissection and immunofluorescence

For timecourse analysis, 3 days before dissection flies were released into DD conditions. Brains were fixed in 15-min windows centred on each reported circadian time (CT), where CT 00/24 is the beginning of the subjective day (lights-on in a 12-h LD cycle). Adult heads were fixed with 4% formaldehyde in phosphate buffer for 1 h at room temperature (RT). Brains were dissected and rinsed in phosphate buffered saline plus 0.1% Triton X-100 (PT) 3 × 15 min. Samples were blocked in 7% normal goat serum for 1 h in PT, incubated with primary antibody at 4 °C for at least 48 h. Primary antibodies were as follows: guinea pig anti-PDF-associated peptide, 1 : 500; rabbit anti-PDF, 1 : 6000 and anti-PER, 1 : 1000; chicken anti-GFP (Upstate Biotechnology) 1/500; mouse anti-βGAL, 1 : 500 (Sigma). Samples were washed in PT 4 × 15 min, and incubated with secondary antibody at 1 : 250 for 2 h at RT; secondary antibodies were washed 4 × 15 min in PT and mounted in 80% glycerol in PT. Secondary antibodies (Jackson ImmunoResearch unless noted) were Cy2- or Cy3-conjugated donkey anti-mouse, Cy2-, Cy3- and Cy5-conjugated donkey antirabbit and Alexa 594 antirat (Invitrogen) and Cy2-antichicken. Embryo and adult immunofluorescence are described in Kidd *et al*. (1998a) and Tayler *et al*. (2004). Anti-ROBO Mab 13C9 was used at 1 : 200 and anti-FasII MAb 1D4 at 1 : 5 (Developmental Studies Hybridoma Bank, Iowa City, IA). Images of coded slides were taken on a Zeiss Pascal confocal microscope. Nuclear and cytoplasmic quantification of PER immunoreactivity was performed employing a Zeiss LSM5 image examiner software. Nuclear PER intensity was calculated as follows: a circle spanning as much nuclear signal as possible was drawn and the signal within it measured; the signal from an equivalent background region within the same focal plane was subtracted. PER intensity within the cytoplasm was determined in a similar fashion (Fernandez *et al*., 2007).

Statistical analysis

Statistical analysis was performed employing the Prism Graphpad 4.0 software package (2003). Average periods for independent genotypes were evaluated employing a one-way ANOVA with a Bonferroni *post hoc* test. In Figs 1B and C and 5A and B, and Supplementary material Table S1, all possible comparisons were performed. In Fig. 4C and I a Student's *t*-test was carried out. The corresponding *P*-values are included in the legend.

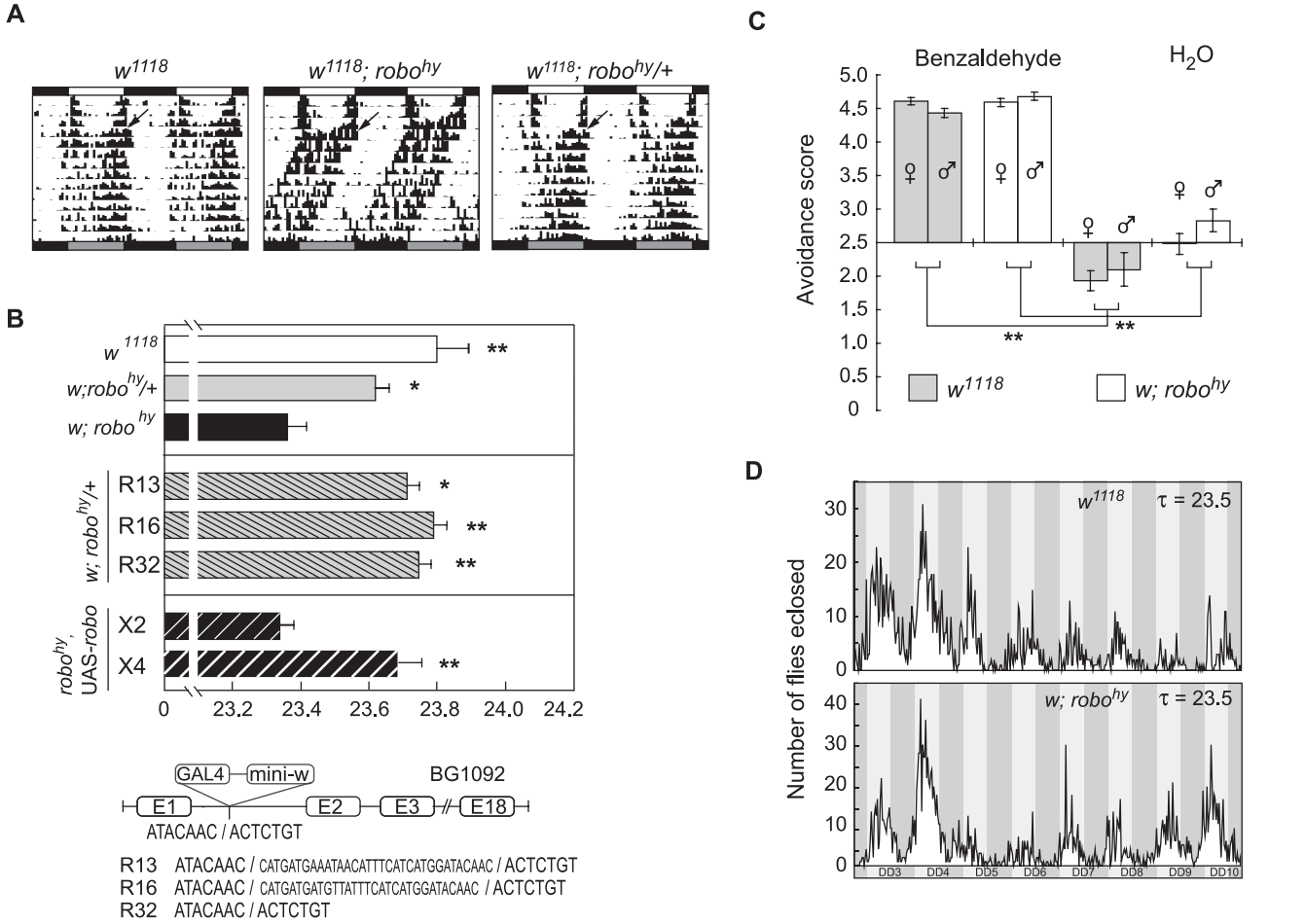

FIG. 1. (A and B) A mutation in *robo* shortened the period of locomotor activity. (A) Representative actograms of control w^{1118}, homozygous and heterozygous $robo^{hy}$. During the experiments, flies were kept in LD for 3 days and then switched to DD (arrow) and monitored for 10 additional days (see supplementary Fig. S1). (B, top panel) Both excision of the P-element and expression of UAS-*robomyc* in the context of $robo^{hy}$ rescued the wild-type phenotype. Locomotor activity experiments were performed as described above. Three independent excised lines (named R13, 16 and 32) were backcrossed to minimize genetic background effects and then tested in the context of a copy of $robo^{hy}$. All of them were different from homozygous $robo^{hy}$ (*$P < 0.05$, **$P < 0.001$) and not different from heterozygous $robo^{hy}$ (one-way ANOVA, with a Bonferroni *post hoc* test). In an independent series of experiments ($n = 3$), overexpression of *UAS-robomyc* in a $robo^{hy}$ homozygous background driven by the GAL 4 in $robo^{hy}$ rescued the short-period phenotype when four copies of *UAS-robomyc* (X4) but not when only two (X2) were expressed in an otherwise identical genetic background, demonstrating that shortening of the period cannot be ascribed to nonspecific background effects. *UAS-robomyc* (X4) was significantly different from homozygous $robo^{hy}$ (**$P < 0.001$, one-way ANOVA, with a Bonferroni *post hoc* test). (B, bottom panel) Schematic diagram of the original P-element insertion (BG1092). R13 and 16 are examples of imprecise excisions (sequence around the insertion point is depicted in the figure) and R32 represents a precise excision. (C) $robo^{hy}$ did not affect aversive olfactory responses. Control and $robo^{hy}$ females and males were tested in groups of five in a quantitative olfactory paradigm (Anholt *et al.*, 1996); left and right panels, respectively; $n = 50$. Ten readings were obtained from each individual group. Experiments were performed twice with similar results (with individual populations), and the average values are shown. Statistical analysis revealed no significant differences between genotypes for both sexes when comparing the response to the odour ($P > 0.05$); the response to benzaldehyde was significantly different from that of water in each group considered (**$P < 0.001$). (D) Eclosion rhythms were not affected by the $robo^{hy}$ mutation. Emergence from the pupal case was recorded every 30 min employing an automated setup (Trikinetics, Waltham, MA, USA). The upper and lower panels represent control ($n = 1789$) and $robo^{hy}$ ($n = 2044$) individuals which emerged from DD 3 to DD 10. Periodogram analysis (Clocklab, Actimetrics) retrieved the endogenous period (τ), which is included in the upper right corner for the experiment shown. The average free-running eclosion period (± SEM) obtained from a minimum of $n = 5$ experiments was 23.7 ± 0.1 h for w^{1118} and 23.8 ± 0.2 h for *w*; $robo^{hy}$. No statistical differences were found. Solid bars indicated subjective days (light grey) and nights (dark grey).

Results

robo Specifically affects locomotor behaviour

Wild-type flies display rhythmic rest–activity cycles concentrating most of their activity around dawn and dusk. When no environmental cues are offered, flies retain this rhythmic activity with a period close to 24 h (Fig. 1A). In search of mutations affecting the period of locomotor activity an insertion potentially affecting the *roundabout* locus was identified, which we named $robo^{hy}$. $robo^{hy}$ homozygous flies showed a consistent and significant shortening of the period of the behavioural rhythm compared to wild-type controls under free-running conditions (DD; Fig. 1A, and supplementary Fig. S1). Heterozygous $robo^{hy}$, on the other hand, exhibited largely normal rhythms.

To rule out genetic background effects on the period phenotype the original P-element insertion was mobilized, and different excised lines were tested for locomotor activity in the context of the $robo^{hy}$ background. Figure 1B shows the period length of three independent excision lines (precise and imprecise, as detailed in the bottom panel) along with the corresponding controls. Two of them still contained ~30 nucleotides from the original P-element within the first intron in the *robo* locus, but this addition did not affect the period of locomotor

activity (supplementary Table S1); in fact, homozygote excisions showed a wild-type period, significantly different from *robo*^{hy}. When tested in the context of a copy of *robo*^{hy} all of them displayed a period not significantly different from heterozygote *robo*^{hy} but different from homozygote *robo*^{hy} (supplementary Table S1), ruling out genetic background effects on the period phenotype.

A rescue experiment was performed to confirm that ROBO is crucial in determining the altered periodicity of the rest–activity cycles, by means of a recombinant *robo*^{hy}, UAS-*robo-mycX2* line. Expression of UAS-*robo-mycX2* from the pattern provided by the gal4 enhancer trap in *robo*^{hy} (Fig. 1B and supplementary Fig. S2) did not rescue the period phenotype when two copies were evaluated (*robo*^{hy}, UAS-*robo-mycX2*/robo^{hy}). However, when the homozygous recombinant line, containing two additional copies of UAS-*robo-myc* was examined, the period approached that of *robo*^{hy}/+ mutants and wild-type controls (Fig. 1B and supplementary Fig. S2), further demonstrating that ROBO function influences the properties of this behaviour.

On the other hand *robo*^{hy} mutants were also examined in an odour-guided behavioural paradigm to rule out nonspecific effects of altered ROBO levels. The avoidance response to benzaldehyde (Anholt *et al*., 1996) was similar between wild-type and mutant flies when employing this quantitative assay (Fig. 1C), thus suggesting that altered periodicity is not a consequence of a pleiotropic neuronal effect resulting from inappropriate levels of ROBO.

robo^{hy} displays normal eclosion behaviour

As ROBO is expressed early in development (Kidd *et al*., 1998a) it was anticipated that this mutation should impact on the rhythmicity of other clock-controlled behaviours. To delve into this issue we characterized the emergence from the puparium, another circadian-regulated behaviour under the control of the PDF circuit (Myers *et al*., 2003), which could manifest ROBO-dependent defects earlier in development. To allow for the narrow period difference to manifest in this population behaviour, pupae were transferred to DD and eclosion was monitored from DD 3 to DD 10. After a week in DD it would be expected than even a small period difference would give rise to a significant change in the average calculated period (Levine *et al*., 2002), or at least cause a shift in the timing of emergence. However, both *w*^{1118} and *robo*^{hy} flies eclosed with a period close to 23.5 h (Fig. 1D), therefore suggesting that the shortening of the period of locomotor behaviour could be attributed to altered ROBO function in the adult brain, or that output circuits controlling eclosion behaviour are spared in *robo*^{hy}.

robo^{hy} *is a hypomorphic allele of* roundabout

Several lines of evidence point to extensive post-transcriptional or -translational regulation of ROBO which underscores the relevance of the absolute levels of this guidance molecule in axon pathfinding (Kidd *et al*., 1998b). The fact that *robo*^{hy} homozygous flies survived through embryogenesis suggested that sufficient ROBO receptor was available during these key early stages of development. To evaluate this possibility we stained the CNS of stage 16 embryos with antibody directed to FASCICLIN II (FAS II), which at this stage specifically labels three longitudinal axon bundles running parallel to the midline (Fig. 2A). Complete loss of function (as in *robo*^{1}; Fig. 2E and I) results in the characteristic 'roundabout' phenotype which named the original mutation (Seeger *et al*., 1993). In *robo*^{null} flies the repulsive SLIT signal is ignored and commissural axons cross the midline repetitively. A single dose of the mutation apparently does not cause any defect (*robo*^{1}/+, Fig. 2D and Kidd *et al*., 1998a), as was the case for *robo*^{hy}/+ flies.

In *robo*^{hy} homozygous mutants the overall pattern of CNS axon scaffold was fairly normal; the longitudinal axon tracts as well as the anterior and posterior commissures were spaced normally and usually had normal thickness. The main defect observed is related to the anterior defasciculation of the longitudinal tracts, whereby in certain segments up to five axonal bundles could be observed (Fig. 2B). In addition, commissural bundles in some segments appeared slightly abnormal and wandered between commissures, extending their projections along and over the midline instead of projecting towards the contralateral side, resulting in a distinct phenotype. Consistent with these observations we found *robo*^{hy}/*robo*^{1} transheterozygotes to share several features of the null alleles, particularly the ectopic crosses (Fig. 2C), which differs from the lack of phenotype observed in *robo*^{1}/+ heterozygous flies. Quantification of the two major defects highlighted that the most prominent one observed in *robo*^{hy} individuals was defasciculation of longitudinal axon bundles, as opposed to what was seen in combination with the null allelic series (Fig. 2F). These results are consistent with a P-insertion directly affecting the *roundabout* locus.

Unlike all previously reported *robo* alleles, *robo*^{hy} is homozygous viable. The P-element insertion affecting *robo* is located in the first intron of the *roundabout* gene within the 5′ untranslated region (Fig. 1B, bottom panel), suggesting alteration of its expression levels (Bellen *et al*., 2004). This observation prompted us to investigate whether the insertion was truly affecting the *robo* locus. Immunohistochemical analysis revealed that the ROBO expression pattern was unaffected in *robo*^{hy} mutant embryos compared to their wild-type counterparts, although the levels of expression clearly appeared compromised (Fig. 2G and H). To determine this difference in ROBO levels, Western blot analysis employing monoclonal ROBO antibodies was performed. A summary quantification of several independent Western blots highlighted that *robo*^{hy} accumulates about half as much ROBO protein as the wild-type controls, in both embryos and adult heads (Fig. 2J and K).

ROBO is expressed in the adult brain neuropil

Previous work regarding ROBO expression in the adult brain led to inconclusive results (Godenschwege *et al*., 2002). One possible explanation for the lack of detection may be the sensitivity of the specific antibodies to the conditions required for fixation. We carried out immunofluorescence on whole-mount adult brains employing an anti-ROBO specific monoclonal antibody (Tayler *et al*., 2004). Under these experimental conditions ROBO signal was widespread and rather diffuse, and decorated several neuropils, particularly within the optic lobe, in regions such as the optic medulla, the lobula plate and the lobula. We also detected signal in the protocerebral bridge, the nodulus, the ellipsoid body and the olfactory lobe. ROBO signal was specifically associated with neuronal projections areas (neuropils; Fig. 3A). Given the short period phenotype of *robo*^{hy} the relationship between ROBO and the PDF circuit was investigated. We found that the small and large somatas of the LNvs are located between ROBO-immunoreactive (-ir) neuropils of the medulla and central brain. The PDF-ir projections running dorsally towards the protocerebrum colocalized with ROBO-ir neuropils in the dorsal protocerebrum (Fig. 3B). We also stained circadian-relevant clusters in the dorsal brain employing *tim-Gal4*; UAS-mCD8-GFP. In the dorsal protocerebrum membrane-bound GFP signal labelled both somas and projections of DN1, 2

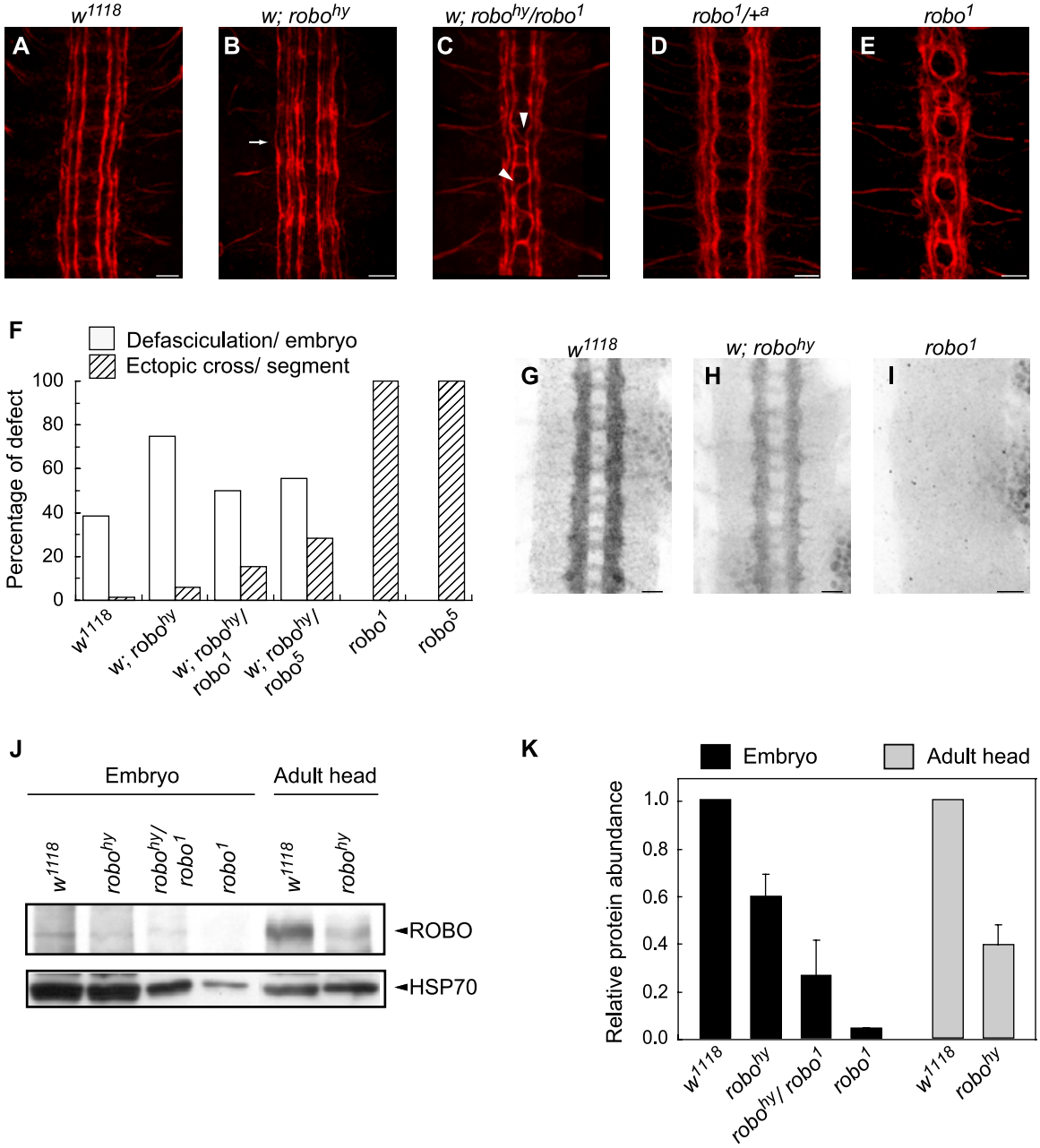

FIG. 2. *robo*^{hy} is a novel adult viable hypomorphic mutant of *roundabout*. (A–E) Panels show four segments of stage 16 embryos with different dosage of *roundabout* stained with anti-FasII antibody. (A) Control *w*^{1118}. (B) *robo*^{hy} mutant showed a less tight axon fasciculation of the longitudinal axons (arrow) and occasional errors in midline guidance. (C) An embryo carrying a copy of *robo*^{hy} and a copy of *robo*^{1}. More severe midline crossing defects are indicated by arrowheads. (D) *robo*^{1}/+^{a} showed neither ectopic crosses nor defasciculation. +^{a} refers to a balancing chromosome known as 'Curly of Oster'. (E) A *robo*^{1}-null mutant displaying clear roundabouts. (F) Percentage of defects associated with different combinations of *robo* alleles. Ectopic crosses per segment are displayed. (G–I) Immunofluorescence revealing that the ROBO endogenous pattern in the embryo was not modified in *robo*^{hy}. Embryo images were taken using the same confocal settings to directly assess ROBO levels in wild-type and mutant genotypes. ROBO staining on a *robo*^{1} null is included as a specificity control. Experiments were performed three or four times with similar results. (J) Western blot analysis of embryo and adult head protein extracts showing that ROBO protein levels were reduced in *robo*^{hy}. Western blots were performed at least four times with independent protein extracts with similar results; a representative experiment is shown. Minor bands of smaller molecular weight were observed, although all of them were also present in *w*^{1118} extracts (data not shown). A *robo*^{1} extract was included as a control for specificity. HSP70 was employed as loading control. (K) Quantification of four (adult head) to seven (embryo) independent experiments is shown. Average normalized values ± SEM for each genotype are depicted in the bar chart. *robo*^{1} extracts were only included in two experiments. Scale bar, 10 μm.

and 3 neurons, as well as the LNds. As expected the somatas were located in a ROBO^{-} region; meanwhile, the axonal projections colocalized with the ROBO signal (Fig. 3C). Immunocytochemical analysis revealed that the ROBO expression pattern appeared unaffected in *robo*^{hy} mutant adults compared to their wild-type counterparts (Fig. 3D), although steady-state levels were strongly reduced, in agreement with the Western blot analysis. Detection of ROBO in the adult brain suggests that it is playing a role at this post-developmental stage. One such possibility would be that ROBO is involved in determining certain synaptic properties of the circuits

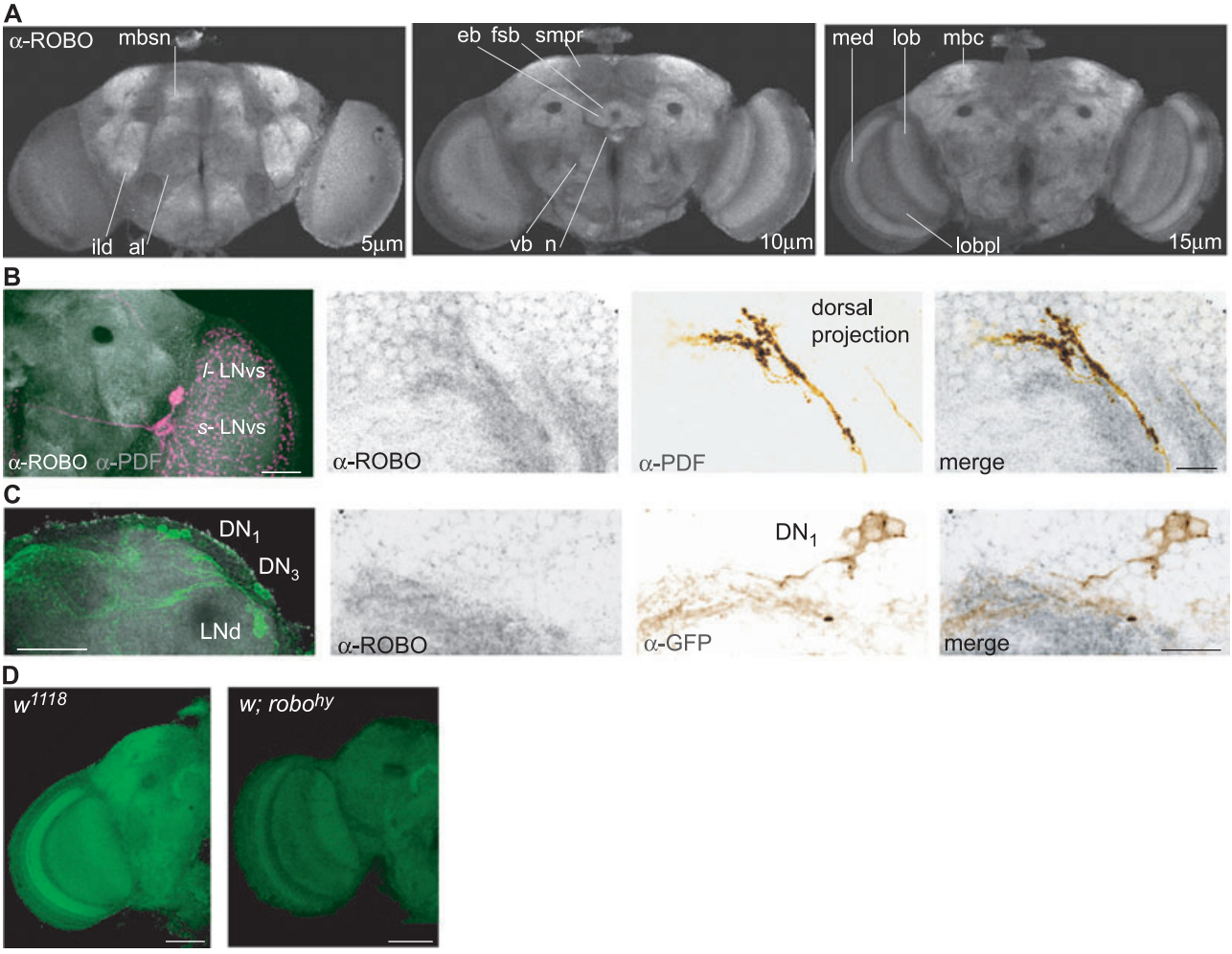

FIG. 3. ROBO was expressed in the adult brain neuropil. (A) Whole-mount brain immunofluorescence with monoclonal anti ROBO antibody revealed the widespread expression pattern of ROBO in the wild-type adult brain (w^{1118}) decorating every neuropil. Frontal scans proceeding from the anterior to the posterior end in the brain allowed the visualization of the mushroom body satellite neuropil (mbsn), the inferior lateral deuterocerebrum (ild), the antennal lobe (al), the ellipsoid body (eb), the ventral body (vb), the fan-shaped body (fsb), the nodulus (n), the lobula (lob), the lobula plate (lobpl), the medulla (med), the mushroom body calyx (mbc) and the superior medial protocerebrum (smpr). Confocal scans of 5 μm taken at different depths are indicated within each figure. (B) Double immunofluorescence to assess ROBO and PDF localization in the adult brain. The first image is a projection of the whole brain (~ 41 μm). Small and large LNv somata appear to be located between ROBO-ir neuropils. On the right, high-magnification views of the dorsalmost segment of the PDF circuit stained with the indicated antibodies (1 μm slices). The image highlights how PDF-ir projections travel within ROBO-ir neuropils. The images were inverted to better assess colocalization (as in C, right panel). (C) Double immunofluorescence to assess ROBO localization in relevant circadian clusters employing *tim-Gal4*; UAS-mCD8-GFP. The image on the left shows a projection from 1 to 21 μm, confirming that the somata are located in ROBO$^-$ areas. The confocal projections correspond to a 1-μm slice through the DN1 cluster stained with anti-ROBO or -GFP antibodies, and the merge shows colocalization between the ROBO-ir neuropils and projections from the DN1s. (D) Immunofluorescence revealing that the ROBO endogenous pattern in the adult brain was not greatly modified in *robo*^{hy}. Images were taken using the same confocal settings used to directly assess ROBO levels in wild-type and *robo*^{hy} genotypes. Experiments were performed three times with similar results. Scale bar, 40 μm except where otherwise indicated.

underlying behaviour, as has been suggested in the giant fibre circuit (Godenschwege *et al*., 2002), or in the maintenance of the neuronal circadian structure.

robo^{hy} *Adult flies exhibit subtle defects in the PDF circuitry*

In the adult fly brain the PDF antibody mainly labels two clusters of neurons, the small and large LNvs, together with their dorsal and contralateral projections (Fig. 4A and D). The integrity of this circuit has been shown to be crucial for robust rhythmic control of locomotor behaviour (Helfrich-Forster, 2003). Given the well documented role of *roundabout* in circuit design during embryogenesis and in the remodeling of the olfactory and visual adult structures (Jhaveri *et al*., 2004; Tayler *et al*., 2004), a thorough analysis of the PDF circuit was undertaken. Whole mount brain immunofluorescence employing anti-PDF antibodies revealed the presence of mislocalized small LNv neurons in roughly half of the *robo*^{hy} brain hemispheres analysed (Fig. 4B and E), which is statistically significantly different from the number observed in the wild-type control (Fig. 4C). Misplaced neurons were located in the dorsal protocerebrum and occasionally were found next to the large LNvs. They appeared to be part of the small LNv cluster as judged by the size of the somas, and by the fact that PER appeared to cycle in phase with the remaining small LNvs; however, their presence in ~30% of wild-type brains (Rieger *et al*., 2006) makes their connection to the shortening of behavioural rhythms unlikely. We have not detected supernumerary cells in any PDF-positive cluster in

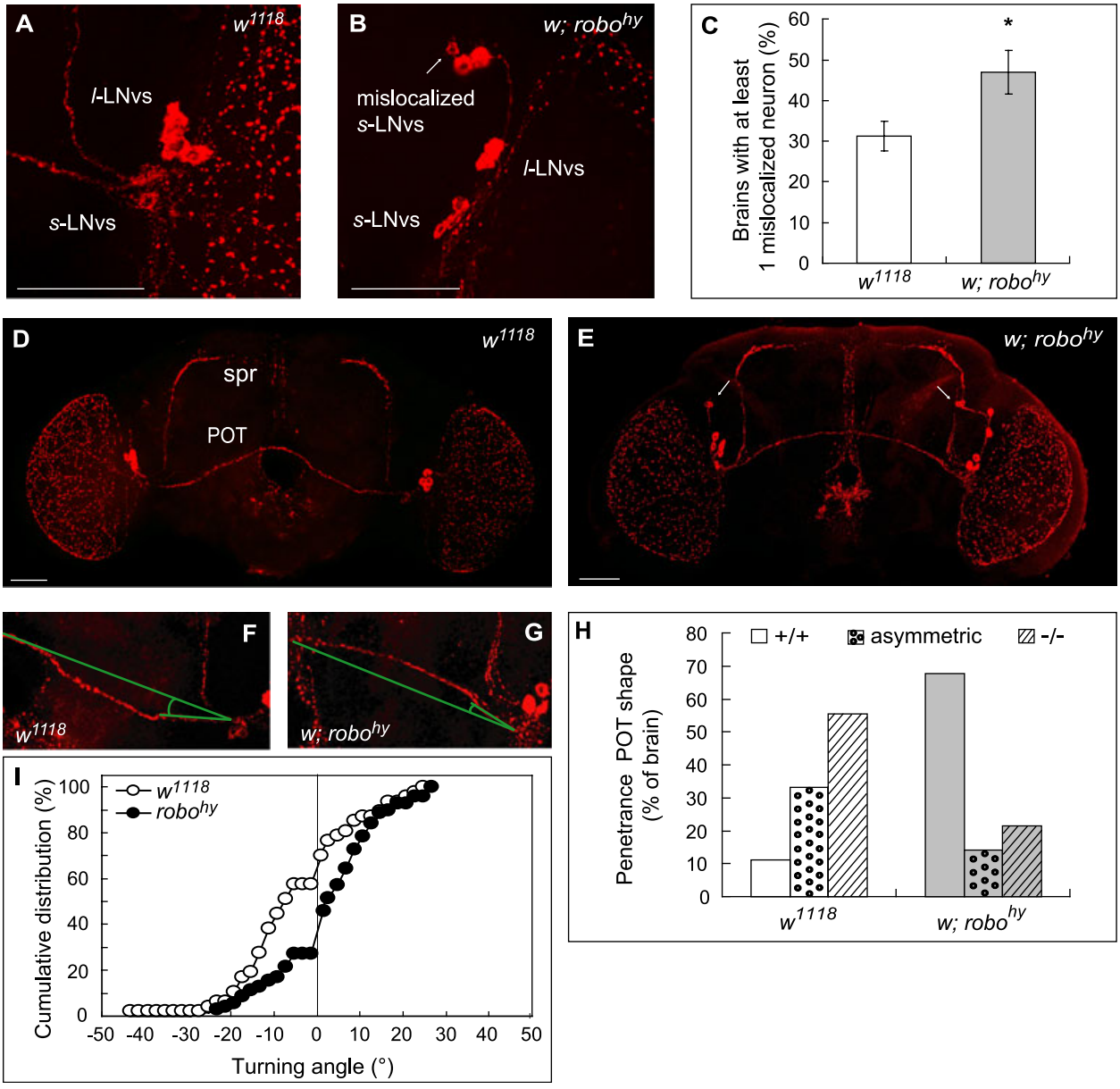

FIG. 4. *robo*^{hy} displayed subtle defects in the PDF circuitry. (A and B) Four small and four large LNvs are stained in a brain hemisphere in w^{1118} and *robo*^{hy}. (B) A mislocalized PDF neuron is observed in *robo*^{hy} (arrow). Ectopic neurons were more dorsal than the large LNvs in the protocerebrum. (C) Percentage of brains showing at least a misplaced neuron. Five experiments were taken into account for the statistical analysis, and a one-tailed Student's *t*-test was performed. *Differences were significant with $P < 0.05$. (D and E) General assessment of the PDF circuitry. The path taken by the projections from the large LNvs running through the POT which connect the large (*l*-LNvs) and small (*s*-LNvs) LNvs from both hemispheres was altered in *robo*^{hy} mutants; spr, superior protocerebrum. Arrows in (E) point to mislocalized neurons. (F and G) Examples of how turning angles were determined in w^{1118} and *robo*^{hy}. (H) Penetrance of the shape in the POT fibers. Brains were separated into three categories: those displaying both hemispheres with positive angles (+/+), both with negative (–/–), or one of each kind (asymmetric). Eighteen brains of w^{1118} and 28 of *robo*^{hy} were considered for the analysis. (I) Cumulative distribution of turning angles in the POT in wild-type and *robo*^{hy} flies. Percentage refers to the proportion of fibers with angular positions lower than a given angle. A Student's *t*-test was employed to compare the average of the two distributions, which showed a significant difference with $P < 0.005$. Scale bar, 40 μm.

robo^{hy}, either. Subtly altered axon trajectories were found in a high proportion of the dissected *robo*^{hy} brains. In-depth observation of the axon bundle running along the posterior optic tract (POT), which has been proposed to connect the large LNvs to the small LNvs on the contralateral side (Kaneko & Hall, 2000), revealed that this projection did not run in the same way as in wild-type brains (Fig. 4D and E). To quantify this difference we measured the angle between the initial turn of the axon fibre and a base line with the same origin that reached an intermediate point in the POT just on top of the esophageal foramen at the midline (Fig. 4F and G). Wild-type brains tended to display 'negative' angles (defined by fibers that would first go down and then turn up as in Fig. 4F), while most *robo*^{hy} brains showed 'positive' angles (defined by fibers that would only go up, as in Fig. 4G). A cumulative frequency distribution highlighted that whereas ~60% of w^{1118} hemispheres exhibited 'negative' angles, only ~30% did so in the mutant background (Fig. 4H and I). Although a slight difference in the axon trajectory resulting from deregulated ROBO levels could interfere with the proper establishment of synapses (Godenschwege *et al.*, 2002), these defects could not solely account for the shortening of the period of

locomotor behaviour as they affect the connection between the large LNvs, whose contribution to the control of behavioural rhythmicity is questionable (Helfrich-Forster, 2003).

robo^{hy} had no effect on the structure of entrainment circuits

Light input to the LNvs relies on both the cell-autonomous *cryptochrome* (Stanewsky *et al*., 1998; Emery *et al*., 2000) and on cues provided by retinal and extraretinal photoreceptors that project directly to these neurons through the optic lobe (Helfrich-Forster *et al*., 2001). ROBO and SLIT have been shown to be relevant in the establishment of the boundaries within the optic lobe (Tayler *et al*., 2004). To examine whether *robo*^{hy} could display subtle alterations in the pattern of axonal navigation conveying resetting cues to the pacemaker centres, whole-mount adult brain immunofluorescence was carried out employing anti-chaoptin, which allows visualization of photoreceptor axons (Van Vactor *et al*., 1988). Wild-type and *robo*^{hy} brains showed no apparent difference in the trajectory of photoreceptor axons at the level of the optic lobe (data not shown). A functional assay was then performed to assess whether light input to the clock could be altered in *robo*^{hy} individuals. Wild-type and *robo*^{hy} flies were synchronized to 12-h LD cycles, and 10-min light pulses were given at zeitgeber time (ZT) 15 and 21 (ZT = 0 indicates the time when lights are switched on) during the dark period of the last LD cycle. Figure 5A shows the phase response to both pulses for the genotypes evaluated. Both wild-type and *robo*^{hy} flies similarly responded to a light pulse during the early night (ZT 15) with an ~3 h phase delay, although the phase shift in mutant flies was larger than in wild-type flies. The opposite appeared to take place after the light pulse at ZT 21: the magnitude of the phase response was slightly smaller in *robo*^{hy} individuals. One possibility to account for these observations is that the accumulation of clock proteins (such as PER and TIM) is advanced in *robo*^{hy} mutants (Yang *et al*., 1998, and see below). These results are consistent with the notion that the period shortening is independent of potential wiring defects on the visual input pathway as an impaired input pathway should similarly affect light pulses given at both time points.

As an independent means to examine pathways for entrainment to the clock, flies synchronized to 12-h LD cycles (in an 08.00–20.00 h regime) were transferred to DD with a 13.00–01.00 h schedule of temperature cycles (25–20 °C, where the warmer temperatures are reminiscent of the light period). After 10 days under synchronizing temperature cycles flies were released into constant conditions and the endogenous period was determined. Figure 5B shows that all genotypes displayed close to 24-h rhythms under temperature entrainment, but the endogenous free-running period was significantly shorter in *robo*^{hy} homozygotes than in wild-type controls.

Overall these data suggest that period shortening is probably not the result of an impairment in the architecture of the input circuits, and point to a requirement for *roundabout* in the circuits underlying rhythmic locomotor behaviour.

ROBO affects signalling downstream of the small LNvs

The period shortening defect displayed by *robo*^{hy} flies is somewhat reminiscent of that of *pdf*^{01} nulls. Mutations affecting PDF (and the PDF receptor) are thought to affect the output signal by which the small LNvs communicate with other tissues, and cause period-shortening and an advanced peak of evening locomotor activity, all hallmarks of *robo*^{hy} (Renn *et al*., 1999; Hyun *et al*., 2005; Lear *et al*., 2005b; Mertens *et al*., 2005). However, most *pdf*^{01} flies become

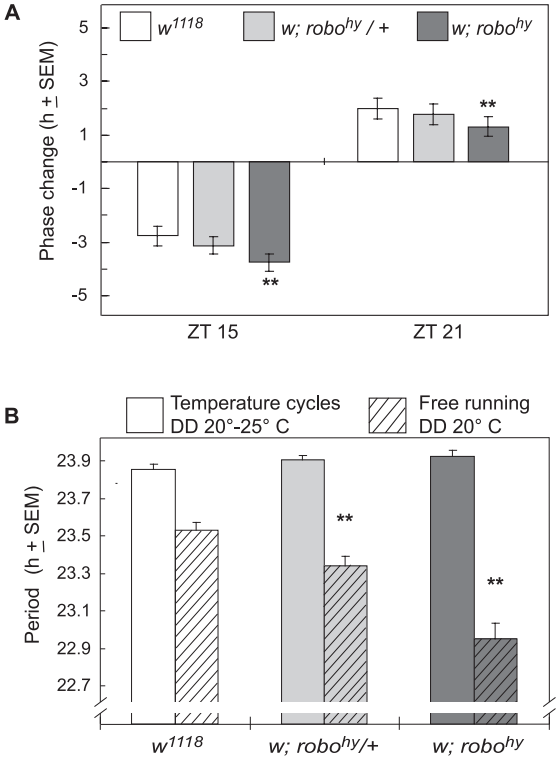

FIG. 5. The mutation in *robo*^{hy} did not affect input pathways. (A) Circadian photosensitivity was retained in the *robo*^{hy} mutant. Phase change of control flies (w^{1118}) as well as heterozygous and homozygous *robo*^{hy} mutants in response to light pulses of 20 μmol/cm^2/s^1 [equivalent to 1400 lux, as in Stanewsky *et al*. (1998)] at ZT 15 and 21. Experiments were performed three times and the average is shown. Phase changes were estimated with respect to the phase of unpulsed controls of the same genotype examined 2 days after the light pulse. Data were pooled from an average of ~50 flies per point. (B) Synchronization to 25–20 °C temperature cycles. Daily and free-running period of flies synchronized to 08.00–20.00 h LD cycles for 3 days that were transferred to a 13.00–01.00 h temperature cycle for 10 days before transfer to DD and constant temperature (20 °C). Experiments were performed three times. Average period for independent genotypes was evaluated employing a one-way ANOVA with a Bonferroni *post hoc* test to compare the free-running period, after temperature cycles, of any given genotype to w^{1118}; $^{**}P < 0.001$.

arrhythmic soon after transfer to constant conditions (Renn *et al*., 1999), while *robo*^{hy} flies are highly rhythmic. These differences suggest that PDF and ROBO operate within distinct mechanisms relevant to the synchronization of output signals from the small LNvs to downstream neurons.

To test whether ROBO could also play a role in output signalling we examined the impact on rest–activity cycles of genetic interactions between *robo*^{hy} and *pdf*^{01} (Fig. 6A and B). Transheterozygotes *robo*^{hy}/+ *pdf*^{01}/+ flies displayed wild-type period and rhythmicity, very similar to the pattern of activity of the individual heterozygotes, suggesting that PDF and ROBO are not necessarily part of the same pathway. However, introducing *robo*^{hy} in *pdf*^{01} lengthened the free-running period in a dose-dependent manner. This result can lead to different interpretations; either the short periodicity remaining in those *pdf*^{01} individuals that stayed rhythmic required wild-type ROBO function or, alternatively, *robo*^{hy} counteracted the signals inducing the short period in *pdf*^{01} mutants.

Most strikingly, introducing a copy of *robo*^{hy} into *pdf*^{01} gave rise to >80% rhythmic individuals. To shed light on the process underlying this increased rhythmicity we analysed the anticipation of the morning and evening peaks in a 12-h LD regime (Fig. 6C). Both w^{1118} and *robo*^{hy} flies displayed a similar morning anticipation, whereas in

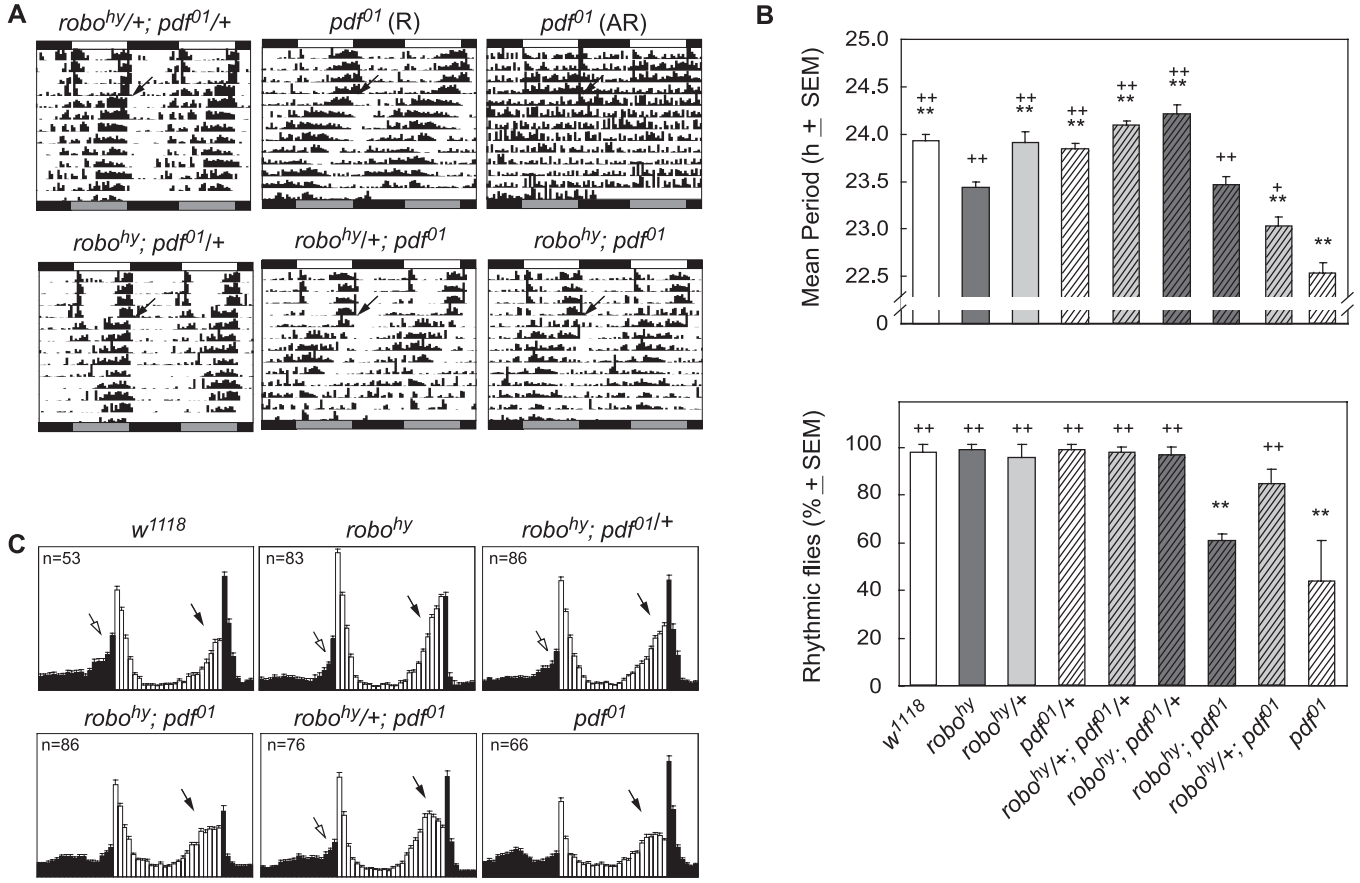

FIG. 6. Genetic interactions between *robo*^{hy} and *pdf*^{01} (see also supplementary Table S2). Locomotor activity was monitored on homozygous and heterozygous *robo*^{hy} in combination with homozygous and heterozygous *pdf*^{01}. (A) Representative actograms of the indicated genotypes. Arrow indicates transfer to DD. (B, upper panel) Period analysis of allelic combinations of *robo*^{hy} and *pdf*^{01} from a representative experiment (of three independent ones) is shown. A χ^2 periodogram analysis was employed (Clocklab). Average periods for independent genotypes were evaluated employing a one-way ANOVA with a Bonferroni *post hoc* test. (B, bottom panel) Percentage of rhythmic flies in the indicated genotypes (the average of three independent experiments is shown). Statistical analysis revealed significant differences with $^{**}P < 0.001$ vs. *robo*^{hy} and $^{++}P < 0.001$ and $^{+}P < 0.01$ vs. *pdf*^{01}. (C) Average activity plots of the indicated genotypes. Data from three independent experiments were analysed. The total number of individuals is shown in the upper left corner. The anticipation of lights on and off transitions are indicated by white and black arrows, respectively.

robo^{hy} the anticipation of the evening transition started at least half an hour earlier than in wild-type controls, consistent with the shorter periodicity in the activity rhythms in free-running conditions. As previously reported, *pdf*^{01} mutants lack the lights-on anticipation while their evening peak is advanced (Renn *et al*., 1999). On the other hand, the average activity plot of *robo*^{hy}/+ *pdf*^{01} flies showed a modest increase in the activity ~1 h before the lights-on transition, indicating that the morning anticipation was rescued even in the absence of PDF neuropeptide (Fig. 6C). The evening anticipation was similar to the *pdf*^{01} line. These data, together with the rescue of free-running rhythmicity, reveal that in *robo*^{hy}/+ *pdf*^{01} flies the circadian network can become synchronized even in the absence of PDF.

Interestingly, reducing *pdf* dosage in the context of *robo*^{hy} only affected rhythmicity in the *robo*^{hy}; *pdf*^{01} double homozygotes, and even those were not as arrhythmic as *pdf*^{01} flies. The average activity plot of these individuals was very similar to the *pdf*^{01} flies, although a subtle increase in activity was observed before lights-on. Furthermore, we noticed that *robo*^{hy}; *pdf*^{01}/+ showed a significantly lengthened period of locomotor activity, indicating that PDF is necessary for the short-period phenotype of *robo*^{hy} to become manifest. Taken together these data suggest that PDF and ROBO could play somewhat complementary functions mediating output signals from the small LNvs to the downstream circadian clusters.

Behavioural defects were associated with shorter molecular oscillations in pacemaker cells

One of the striking features of the *robo*^{hy} mutant lines was the shortening of the locomotor activity rhythms.

To directly account for the pace of the intracellular molecular clock we followed PER accumulation in the small LNvs. Newly eclosed *w*^{1118} and *robo*^{hy} adult flies were synchronized to 5 days in LD. Double-immunofluorescence experiments were performed to follow PER and PDF accumulation on the third day upon transfer to continuous darkness (DD 3).

In the small LNvs of *w*^{1118} flies (supplementary Fig. S3, top panel) PER was found primarily in the nucleus at CT 0. PER nuclear levels decreased during the subjective morning and became undetectable by CT 9. At CT 15 PER was detected in the cytoplasm colocalizing with the cytoplasmic PDF signal; by CT 18 it was detected in both the cytoplasm and nucleus, to become mostly nuclear again by CT 21. In *robo*^{hy} mutants (bottom panel) PER was also nuclear at CT 0 and CT 3, barely detectable at CT 6 and undetectable by CT 9. In contrast to *w*^{1118} flies, however, PER cytoplasmic levels rose by CT 12 and became fully nuclear by CT 18.

To better assess PER accumulation within the cytoplasm and its entrance to the nucleus, its localization was examined focusing on the

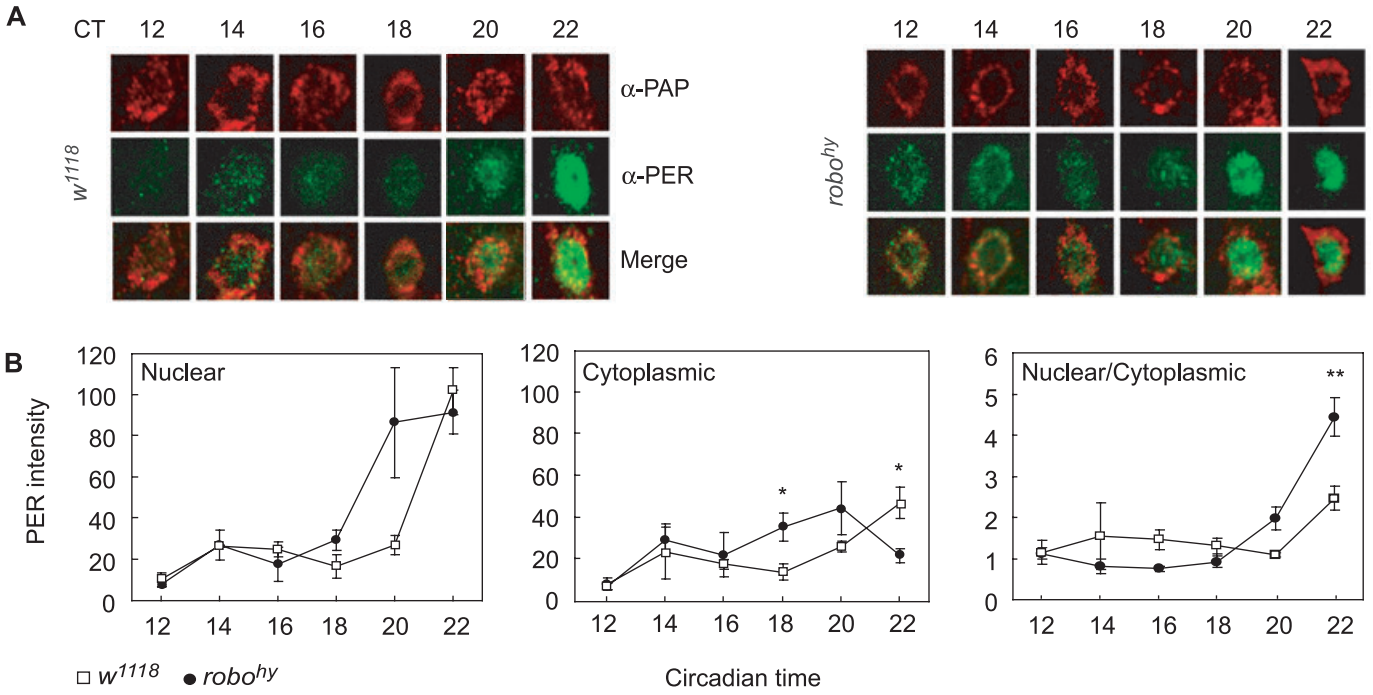

FIG. 7. Molecular oscillations in the small LNvs were affected in *robo*^{hy}. (A) Newly eclosed w^{1118} and *robo*^{hy} adult flies were synchronized and samples were taken every 2 h during subjective night in DD 3. Whole-mount brain immunofluorescence was performed to follow PDF-associated peptide (PAP; upper panel) and PER (middle) accumulation in wild-type and *robo*^{hy} brains. Images are a reconstruction of one or two sections, and were taken employing the same confocal settings for each individual timecourse. The experiment was performed three times with similar results. (B) The plots display the changes in PER intensity in the nucleus and cytoplasm as well as the ratio of nuclear to cytoplasmic PER intensity at each timepoint for w^{1118} and *robo*^{hy}. Each value represents the average of the sLNvs ($n = 4$–10). Images and quantification were performed blind. Statistical analysis revealed significant differences with $^{**}P < 0.001$ and $^{*}P < 0.05$ at the timepoints indicated in the Figure.

subjective night with higher time resolution (Fig. 7). Under these conditions PER was detectable within the cytoplasm at CT 12 in *robo*^{hy} (Fig. 7A, right panel), while in control brains it was only seen by CT 14 (left panel). Likewise, the PER signal was exclusively nuclear by CT 20 although it had not fully entered the nucleus by CT 22 in w^{1118} flies.

To quantify the differences in PER subcellular distribution, the nuclear and cytoplasmic intensity of the PER signal was determined and the ratio was calculated. This measurement does not allow for direct comparisons on PER levels between genotypes but should provide an independent means to evaluate PER nuclear entry. As shown in Fig. 7B, nuclear PER was detected sooner in *robo*^{hy} than in w^{1118} flies (left and middle panels) as nuclear intensity reached its maximum by CT 20 in *robo*^{hy} while in wild-type flies it did so by CT 22, so that the N : C ratio was still growing at CT 22.

In sum, advanced PER entry to the nucleus in *robo*^{hy} individuals is consistent with the period shortening of overt rhythms observed in locomotor activity, suggesting that either this shortened molecular oscillations are initiated within the small LNvs or altered communication within the circadian network could impinge on the pace of the molecular oscillations in this cluster.

Discussion

Reduced ROBO levels subtly altered the architecture of circadian circuits

In *Drosophila* ROBO has extensively been shown to participate in guiding axon pathfinding through the midline during the development of the embryonic CNS (Seeger *et al*., 1993; Kidd *et al*., 1998a; Kidd *et al*., 1999) as well as positioning sensory terminals in the olfactory lobe (Jhaveri *et al*., 2004) and proper compartimentalization of the visual system (Tayler *et al*., 2004) in the early pupa. However, the absence of ROBO did not cause any anatomical defects in the development of the central complex taking place during metamorphosis, unlike what was seen for ROBO 2 and 3 (Nicolas & Preat, 2005). We anticipated that a hypomorphic mutation in *robo* could affecct the configuration or correct placement of PDF-ir cells and/or their projections, thereby impinging upon behavioural rhythms. Among the PDF-ir cells the small LNvs are usually clustered and persist without any morphological changes throughout adulthood; meanwhile, the large LNvs can often be found in different arrangements in wild-type flies (as described in detail in Helfrich-Forster, 1997). Surprisingly, the small LNvs were found in altered locations in a fraction of *robo*^{hy} mutants as well as in wild-type brains (Fig. 4 and Rieger *et al*., 2006); in fact about half of *robo*^{hy} brains showed ectopic small LNvs whilst >95% of them were still strongly rhythmic, thus undermining the impact of mislocalized somas over rhythmic activity. Another feature of the *robo*^{hy} mutant brains relates to the trajectory of the contralateral projections of the large LNvs running through the POT. A difference was observed between wild-type and *robo*^{hy} mutants whose trajectory turned out to be significantly different between the two genotypes (Fig. 4J). Although these defects are probably due to reduced ROBO levels, neither of them fully account for the highly penetrant shortening of the behavioural rhythms (supplementary Fig. S1). Notwithstanding, even slight changes in the structure of the circadian network could give rise to subtle defects in the connectivity of the underlying circuit, eventually impinging upon overt behaviour.

How could ROBO affect rhythmic rest–activity cycles?

One possibility to account for the shortened molecular rhythms would be that distorted ROBO signalling altered the cellular balance leading to changes in molecular oscillations, for example by altering protein phosphorylation controlling PER/TIM entrance to the nucleus, which would rely on proteins involved in ROBO's transduction cascade to be present in pacemaker cells. This explanation would imply that ROBO is not *per se* involved in rhythmic control of behaviour, but subtle alterations in key components of ROBO signalling would play a role within the cell-autonomous oscillator.

An alternative mechanism to explain the circadian defect is based on the proposed synchronizing effect of the contralateral projections (a hypothesis based purely on the anatomical description: (Kaneko & Hall, 2000). If projections from the large LNvs were meant to provide synchronizing signals to the contralateral small LNvs then it would be reasonable to expect that altered synaptic connectivity due to constantly reduced ROBO levels in the adult brain could convey slightly modified synchronizing signals. However, we could not find any evidence of desynchronization in PER subcellular localization between hemispheres in the small LNvs, even at DD 6 (unpublished observations).

We favour the notion that distorted neuronal activity caused by defective synaptic contacts in any component of the circadian network could in turn impinge upon the molecular oscillations in the small LNvs. Our results showed that $robo^{hy}$ mutants displayed a short period in locomotor activity even though the period of eclosion (another clock-controlled behaviour) was spared (Fig. 1D). However, both behaviours appear to be under the control of the small LNvs (Myers *et al*., 2003), whose molecular oscillations were advanced in $robo^{hy}$ adult flies (Fig. 7 and supplementary Fig. S3). This apparent discrepancy suggests that either locomotor and eclosion behaviours are not equally sensitive to changes in the properties of the underlying circuits, or that shortening of the period of rest–activity cycles results from an altered circadian circuitry in the adult. During metamorphosis new circadian clusters develop (Helfrich-Forster, 1997; Kaneko & Hall, 2000); these may not participate in the functional network until after adult eclosion, thus explaining the lack of effect on this rhythm; in this view, period shortening in locomotor behaviour would be the consequence of an altered communication between the novel clusters and the small LNvs, potentially derived from developmental defects affecting axon wiring or synaptogenesis. Indeed, Godenschwege and colleagues have already demonstrated that altering ROBO levels in the giant fibre affects synaptic connectivity (Godenschwege *et al*., 2002). Moreover, Nitabach *et al*. (2002) showed that altering the electric properties of the PDF circuit affects both the molecular oscillator and rhythmic behaviour (Nitabach *et al*., 2002). Thus, in $robo^{hy}$ the period change would not be initiated within the small LNvs but rather result from the interaction of the entire circadian network in the adult brain in which ROBO is present (such as the projections from DNs and LNds; Fig. 3C). In fact, anatomical data suggesting there is a direct contact between dorsal clusters and the small LNvs was recently reported (Stoleru *et al*., 2004; Helfrich-Forster *et al*., 2007). Furthermore, Stoleru *et al*. (2004) showed that lack of a functional clock in the small LNvs did not preclude production of a morning peak in LD, suggesting a coupling between the two groups of cells.

The unexpected intermediate phenotypes observed along the course of the genetic interactions with PDF underscores the complexity of the underlying mechanisms. We envision at least two possibilities. If reduced ROBO levels altered the balance of neuropeptide release, the communication among the small LNvs and/or between them and their postsynaptic targets would be affected, resulting in a defective output (Peng *et al*., 2003; Lin *et al*., 2004; Stoleru *et al*., 2005). A decrease in PDF levels in $robo^{hy}$ mutants induced lengthening of the period of locomotor activity, suggesting that period depends on PDF levels. This observation is not unprecedented; in fact it has been reported that PDF miss-expression induced period changes as well as altered rhythmicity (Helfrich-Forster, 2000). In this case a very extreme phenotype would be similar to that of the pdf^{01} mutants; this could apparently be the case in $robo^{hy}$ individuals, as they become progressively arrhythmic as they age (J. Beckwith and M. Fernanda Ceriani, unpublished observations). On the other hand, defective ROBO function could lead to altered cell-to-cell contacts (Rhee *et al*., 2002). Recently Schneider and Stengl demonstrated that subpopulations of neurons connected through gap junctions impart synchronizing cues to circadian oscillators in the accessory medulla in the cockroach (Schneider & Stengl, 2005, 2006), suggesting that affected cell-to-cell contacts could in part account for the defects in $robo^{hy}$.

The observation that ROBO function could modulate the properties of the molecular clock clearly affects our understanding of the underlying processes, particularly in light of the conservation of the two pathways between flies and mice.

Supplementary material

The following supplementary material may be found on http://www.blackwell-synergy.com

Fig. S1. Altered ROBO levels affected the period of rhythmic behavior.

Fig. S2. Overexpression of *robo* rescues the short period phenotype in a dose-dependent manner.

Fig. S3. Molecular oscillations in the small LNvs are affected in $robo^{hy}$.

Table S1. Removal of the P element rescues the short period phenotype.

Table S2. Genetic interactions between $robo^{hy}$ and pdf^{01}.

Please note: Blackwell Publishing are not responsible for the content or functionality of any supplementary materials supplied by the authors. Any queries (other than missing material) should be directed to the correspondence author for the article.

Acknowledgements

We are indebted to S Lavista-Llanos and L Centanin for helpful discussions and to A Schinder, G Corfas and V Gottifredi for critical reading of the manuscript. We thank C Helfrich-Forster and M Rosenzweig for advice on immunofluorescence. We also thank G Tear for his $robo^{null}$ allelic series, R Murphey for the UAS-*robo-myc*2X, O Shafer for pdf^{01} and K Matthews and the Bloomington Stock Center for fly stocks. We are also grateful to J Hall and F Rouyer for anti-PDF antibodies, P Taghert for anti-PDF-associated peptide, and M Rosbash for anti-PER antibody. The anti-ROBO 13C9 and anti-Fas II ID4 were obtained from the Developmental Studies Hybridoma Bank. M.F.C. is a member of the Argentine Research Council (CONICET). J.B., E.B. and M.P.F. are supported by a graduate fellowship from CONICET. This work was supported by a startup grant from The PEW Charitable Foundation, a re-entry grant from Fundación Antorchas and the HHMI International Research Program (n°55003668) to M.F.C.

Abbreviations

CT, circadian time; DD, constant darkness; DN, dorsal neuron; GFP, green fluorescent protein; ir, immunoreactive; LD, light–dark; LNd, lateral neuron dorsal; LNv, ventral lateral neuron; PDF, pigment-dispersing factor; PER, PERIOD; POT, posterior optic tract; *robo*, *roundabout*; $robo^{hy}$, $robo^{hypomorph}$; ZT, zeitgeber time.

References

Anholt, R.R., Lyman, R.F. & Mackay, T.F. (1996) Effects of single P-element insertions on olfactory behavior in Drosophila melanogaster. *Genetics*, **143**, 293–301.

Bellen, H.J., Levis, R.W., Liao, G., He, Y., Carlson, J.W., Tsang, G., Evans-Holm, M., Hiesinger, P.R., Schulze, K.L., Rubin, G.M., Hoskins, R.A. & Spradling, A.C. (2004) The BDGP gene disruption project: single transposon insertions associated with 40% of Drosophila genes. *Genetics*, **167**, 761–781.

Ceriani, M.F., Hogenesch, J.B., Yanovsky, M., Panda, S., Straume, M. & Kay, S.A. (2002) Genome-wide expression analysis in Drosophila reveals genes controlling circadian behavior. *J. Neurosci.*, **22**, 9305–9319.

Emery, P., Stanewsky, R., Helfrich-Forster, C., Emery-Le, M., Hall, J.C. & Rosbash, M. (2000) Drosophila CRY is a deep brain circadian photoreceptor. *Neuron*, **26**, 493–504.

Fernandez, M.P., Chu, J., Villella, A., Atkinson, N., Kay, S.A. & Ceriani, M.F. (2007) Impaired clock output by altered connectivity in the circadian network. *Proc. Natl Acad. Sci. USA*, **104**, 5650–5655.

Godenschwege, T.A., Simpson, J.H., Shan, X., Bashaw, G.J., Goodman, C.S. & Murphey, R.K. (2002) Ectopic expression in the giant fiber system of Drosophila reveals distinct roles for roundabout (Robo), Robo2, and Robo3 in dendritic guidance and synaptic connectivity. *J. Neurosci.*, **22**, 3117–3129.

Goodman, C.S. (1996) Mechanisms and molecules that control growth cone guidance. *Annu. Rev. Neurosci.*, **19**, 341–377.

Hardin, P.E. (2005) The circadian timekeeping system of Drosophila. *Curr. Biol.*, **15**, R714–R722.

Helfrich-Forster, C. (1997) Development of pigment-dispersing hormone-immunoreactive neurons in the nervous system of Drosophila melanogaster. *J. Comp. Neurol.*, **380**, 335–354.

Helfrich-Forster, C. (1998) Robust circadian rhythmicity of Drosophila melanogaster requires the presence of lateral neurons: a brain-behavioral study of disconnected mutants. *J. Comp. Physiol. [a]*, **182**, 435–453.

Helfrich-Forster, C. (2003) The neuroarchitecture of the circadian clock in the brain of Drosophila melanogaster. *Microsc. Res. Tech.*, **62**, 94–102.

Helfrich-Forster, C., Shafer, O.T., Wulbeck, C., Grieshaber, E., Rieger, D. & Taghert, P. (2007) Development and morphology of the clock-gene-expressing lateral neurons of Drosophila melanogaster. *J. Comp. Neurol.*, **500**, 47–70.

Helfrich-Forster, C., Tauber, M., Park, J.H., Muhlig-Versen, M., Schneuwly, S. & Hofbauer, A. (2000) Ectopic expression of the neuropeptide pigment-dispersing factor alters behavioral rhythms in Drosophila melanogaster. *J. Neurosci.*, **20**, 3339–3353.

Helfrich-Forster, C., Winter, C., Hofbauer, A., Hall, J.C. & Stanewsky, R. (2001) The circadian clock of fruit flies is blind after elimination of all known photoreceptors. *Neuron*, **30**, 249–261.

Hyun, S., Lee, Y., Hong, S.T., Bang, S., Paik, D., Kang, J., Shin, J., Lee, J., Jeon, K., Hwang, S., Bae, E. & Kim, J. (2005) Drosophila GPCR Han is a receptor for the circadian clock neuropeptide PDF. *Neuron*, **48**, 267–278.

Jhaveri, D., Saharan, S., Sen, A. & Rodrigues, V. (2004) Positioning sensory terminals in the olfactory lobe of Drosophila by Robo signaling. *Development*, **131**, 1903–1912.

Kaneko, M. & Hall, J.C. (2000) Neuroanatomy of cells expressing clock genes in Drosophila: transgenic manipulation of the period and timeless genes to mark the perikarya of circadian pacemaker neurons and their projections. *J. Comp. Neurol.*, **422**, 66–94.

Kidd, T., Bland, K.S. & Goodman, C.S. (1999) Slit is the midline repellent for the robo receptor in Drosophila. *Cell*, **96**, 785–794.

Kidd, T., Brose, K., Mitchell, K.J., Fetter, R.D., Tessier-Lavigne, M., Goodman, C.S. & Tear, G. (1998a) Roundabout controls axon crossing of the CNS midline and defines a novel subfamily of evolutionarily conserved guidance receptors. *Cell*, **92**, 205–215.

Kidd, T., Russell, C., Goodman, C.S. & Tear, G. (1998b) Dosage-sensitive and complementary functions of roundabout and commissureless control axon crossing of the CNS midline. *Neuron*, **20**, 25–33.

Kramer, S.G., Kidd, T., Simpson, J.H. & Goodman, C.S. (2001) Switching repulsion to attraction: changing responses to slit during transition in mesoderm migration. *Science*, **292**, 737–740.

Lear, B.C., Lin, J.M., Keath, J.R., McGill, J.J., Raman, I.M. & Allada, R. (2005a) The ion channel narrow abdomen is critical for neural output of the Drosophila circadian pacemaker. *Neuron*, **48**, 965–976.

Lear, B.C., Merrill, C.E., Lin, J.M., Schroeder, A., Zhang, L. & Allada, R. (2005b) A G protein-coupled receptor, groom-of-PDF, is required for PDF neuron action in circadian behavior. *Neuron*, **48**, 221–227.

Levine, J.D., Funes, P., Dowse, H.B. & Hall, J.C. (2002) Signal analysis of behavioral and molecular cycles. *BMC Neurosci.*, **3**, 1.

Lin, Y., Stormo, G.D. & Taghert, P.H. (2004) The neuropeptide pigment-dispersing factor coordinates pacemaker interactions in the Drosophila cricadian system. *J. Neurosci.*, **24**, 7951–7957.

Mertens, I., Vandingenen, A., Johnson, E.C., Shafer, O.T., Li, W., Trigg, J.S., De Loof, A., Schoofs, L. & Taghert, P.H. (2005) PDF receptor signaling in Drosophila contributes to both circadian and geotactic behaviors. *Neuron*, **48**, 213–219.

Myers, E.M., Yu, J. & Sehgal, A. (2003) Circadian control of eclosion: interaction between a central and peripheral clock in Drosophila melanogaster. *Curr. Biol.*, **13**, 526–533.

Nicolas, E. & Preat, T. (2005) Drosophila central brain formation requires Robo proteins. *Dev. Genes Evol.*, **215**, 530–536.

Nitabach, M.N., Balu, J. & Holmes, T.C. (2002) Electrical silencing of Drosophila pacemaker neurons stops the free-running circadian clock. *Cell*, **109**, 485–495.

Park, J.H., Helfrich-Forster, C., Lee, G., Liu, L., Rosbash, M. & Hall, J.C. (2000) Differential regulation of circadian pacemaker output by separate clock genes in Drosophila. *Proc. Natl Acad. Sci. USA*, **97**, 3608–3613.

Peng, Y., Stoleru, D., Levine, J.D., Hall, J.C. & Rosbash, M. (2003) Drosophila free-running rhythms require intercellular communication. *PLoS Biol.*, **1**, E13.

Rajagopalan, S., Nicolas, E., Vivancos, V., Berger, J. & Dickson, B.J. (2000) Crossing the midline: roles and regulation of Robo receptors. *Neuron*, **28**, 767–777.

Renn, S.C., Park, J.H., Rosbash, M., Hall, J.C. & Taghert, P.H. (1999) A pdf neuropeptide gene mutation and ablation of PDF neurons each cause severe abnormalities of behavioral circadian rhythms in Drosophila. *Cell*, **99**, 791–802.

Rhee, J., Mahfooz, N.S., Arregui, C., Lilien, J., Balsamo, J. & VanBerkum, M.F. (2002) Activation of the repulsive receptor Roundabout inhibits N-cadherin-mediated cell adhesion. *Nat. Cell. Biol.*, **4**, 798–805.

Rieger, D., Shafer, O.T., Tomioka, K. & Helfrich-Forster, C. (2006) Functional analysis of circadian pacemaker neurons in Drosophila melanogaster. *J. Neurosci.*, **26**, 2531–2543.

Schneider, N.L. & Stengl, M. (2005) Pigment-dispersing factor and GABA synchronize cells of the isolated cricadian clock of the cockroach *Leucophaea maderae*. *J. Neurosci.*, **25**, 5138–5147.

Schneider, N.L. & Stengl, M. (2006) Gap junctions between accessory medulla neurons appear to synchronize circadian clock cells of the cockroach *Leucophaca maderae*. *J. Neurophysiol*, **95**, 1996–2002.

Seeger, M., Tear, G., Ferres-Marco, D. & Goodman, C.S. (1993) Mutations affecting growth cone guidance in Drosophila: genes necessary for guidance toward or away from the midline. *Neuron*, **10**, 409–426.

Simpson, J.H., Kidd, T., Bland, K.S. & Goodman, C.S. (2000) Short-range and long-range guidance by slit and its Robo receptors. Robo and Robo2 play distinct roles in midline guidance. *Neuron*, **28**, 753–766.

Stanewsky, R., Kaneko, M., Emery, P., Beretta, B., Wager-Smith, K., Kay, S.A., Rosbash, M. & Hall, J.C. (1998) The cryb mutation identifies cryptochrome as a circadian photoreceptor in Drosophila. *Cell*, **95**, 681–692.

Stoleru, D., Peng, Y., Agosto, J. & Rosbash, M. (2004) Coupled oscillators control morning and evening locomotor behaviour of Drosophila. *Nature*, **431**, 862–868.

Stoleru, D., Peng, Y., Nawathean, P. & Rosbash, M. (2005) A resetting signal between Drosophila pacemakers synchronizes morning and evening activity. *Nature*, **438**, 238–242.

Tayler, T.D., Robichaux, M.B. & Garrity, P.A. (2004) Compartmentalization of visual centers in the Drosophila brain requires Slit and Robo proteins. *Development*, **131**, 5935–5945.

Van Vactor, D.L., Krantz, D.E., Reinke, R. & Zipursky, S.L. (1988) Analysis of mutants in chaoptin, a photoreceptor cell-specific glycoprotein in Drosophila, reveals its role in cellular morphogenesis. *Cell*, **52**, 281–290.

Yang, Z., Emerson, M., Su, H.S. & Sehgal, A. (1998) Response of the timeless protein to light correlates with behavioral entrainment and suggests a non-visual pathway for circadian photoreception. *Neuron*, **21**, 215–223.

Yang, Z. & Sehgal, A. (2001) Role of molecular oscillations in generating behavioral rhythms in Drosophila. *Neuron*, **29**, 453–467.